

# MODELING THE SEASONAL VARIABILITY OF THE H<sub>2</sub>O VAPOR AND ICE CLOUDS IN THE MARTIAN ATMOSPHERE.

G. Machtoub, A. Medvedev, P. Hartogh, *Max Planck Institute for Solar System Research, Katlenburg-Lindau, Germany (machtoub@mps.mpg.de).*

## Introduction

A few studies have focused on the spatial distribution of high-altitude water ice clouds, and vapor outbursts in the northern and southern polar regions of Mars. Recent GCM simulations have indicated that the temporal variability of the migrated H<sub>2</sub>O vapor and water ice clouds plays an important role in the Martian water cycle. Several cloud parameterization have successfully modeled the Martian H<sub>2</sub>O cycle, but there still exist considerable discrepancies between the published GCM simulations and observations [Heavens *et al.*, 2010; McCleese, *et al.*, 2010; Smith *et al.*, 2001]. The simulated water ice clouds over the northern tropics were predicted thicker and lower than shown in the observations by the Mars Climate Sounder (MCS) on Mars Reconnaissance Orbiter. This may also underestimate the intensity of the meridional circulation at higher altitudes.

In this work, we investigate water cycle with a recent version of the MAOAM-GCM [Hartogh *et al.*, 2005]. The current version incorporates a self-consistent H<sub>2</sub>O cycle. The model employs a new spectral solver [Becker *et al.*, 2009] and a number of parameterizations for the microphysical processes taking into account the transport of two dynamical tracers: H<sub>2</sub>O vapor and ice. The present simulations are focused on the validation of the newly developed microphysical scheme and intended to investigate the upward flux of H<sub>2</sub>O vapor, and the local time trends of the ice clouds. The model simulations are compared with recent Martian observations.

## Model description

The model incorporates the H<sub>2</sub>O cycle by defining the water source and parameterizing a combination of microphysical processes, involving ground ice sublimation, cloud formation and ice surface deposition. The variable particle size distribution is used in describing these processes. Seasonal and spatial distributions of water are controlled by the transport and condensation of water vapor and the sublimation of water ice. During each time step, a heterogeneous condensation controls the growth, and sublimation of ice by the saturation vapor pressure influenced by changes in the temperature and the ice particle radius. The sublimation flux is sensitive to the temperature of the residual cap, which controls the global moisture abundances [Richardson *et al.*, 2002]. When the atmospheric temperature is low enough and the air is supersaturated, the excess of water

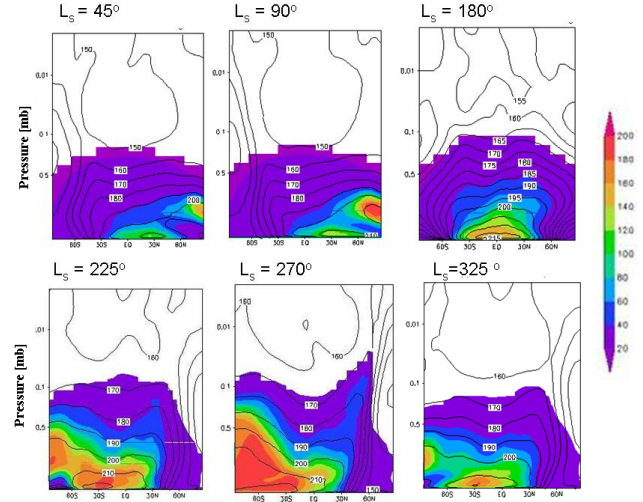


Figure 1: Simulated cross sections of the zonally averaged mass mixing ratios of water vapor [ppm] (shaded) and temperature [K] (contours) for one Martian year at  $L_s=45^\circ$ ,  $90^\circ$ ,  $180^\circ$ ,  $225^\circ$ ,  $270^\circ$ , and  $325^\circ$

vapor is condensed back onto ice. The simulations described below were performed at T21 spectral resolution ( $64 \times 32$  grid points in longitude and latitude) on 50 vertical levels. The vertical grid is given by hybrid coordinates, which reduce to terrain-following  $\sigma$ -coordinates in the lower atmosphere, and to pressure levels at the upper layers. The top of the model domain is set at approximately 120 km. The model also includes realistic topography, albedo and thermal inertia distributions at the surface, CO<sub>2</sub> condensation/sublimation processes, and accounts for radiative heating and cooling by the CO<sub>2</sub> gas and atmospheric dust in visible and infrared wavelengths.

## Simulations

The initial vertical and horizontal distribution of water vapor has been introduced after the initial spin-up of the GCM, taking into account the presence of the residual water ice cap, which consists of an initial amount of water ice centered on the northern pole northward of 82 N. The model is run for one Martian year. The simulations are started with an isothermal (200 K) and windless state at the aphelion. The amount of dust has

been prescribed and kept constant throughout the current simulations under clear atmospheric conditions with the dust optical depth  $\tau = 0.2$ .

During late solstice seasons, the upward flux of the subliming water from the polar caps substantially increases in the Northern hemisphere near  $L_s = 125^\circ - 145^\circ$  and in the Southern hemisphere near  $L_s = 225^\circ - 275^\circ$ . Our first results on water cycle simulations for an entire Martian year are presented in Figure 1. The simulations of the zonally averaged mass mixing ratios of water vapor for selected seasons ( $L_s = 45^\circ, 90^\circ, 180^\circ, 225^\circ, 270^\circ, 325^\circ$ ) highlight the response of the water vapor to the temperature and meridional circulation. The simulated hygropause, which marks the highest point from where water vapor rapidly decreases, has a well-defined latitudinal structure (shown by the shading). The model is in a good agreement with observations and compares well with other GCM simulations [Richardson *et al.*, 2002, Montmessin *et al.*, 2004; Moudden *et al.*, 2007]. The water vapor substantially varies on short time

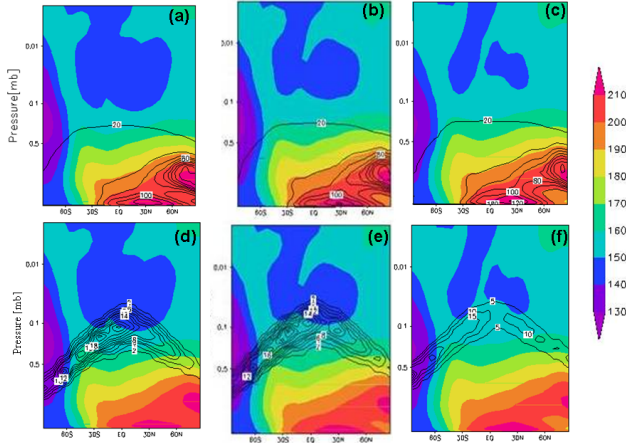


Figure 2: Zonally averaged temperature [K] (shaded) and mass mixing ratios [ppm] (contours) of water vapor (a-c) and ice clouds (d-f) at  $L_s = 110^\circ, 120^\circ$ , and  $140^\circ$ , respectively.

scales during late spring and early summer. The strong contribution of planetary waves to the water cycle is well established in the spatial distribution of water vapor and ice clouds in mid-latitudes. High-altitude ice clouds are formed over the Martian tropics during northern summer due to subsequent advection by upper branches of the Hadley cell. Figure 2 shows the simulated mass mixing ratios of the water vapor and ice clouds for  $L_s = 110^\circ - 140^\circ$ . Our predicted mass mixing ratios of water ice clouds are well consistent with the ratios derived from MCS retrievals by Heavens *et al.* [2010]. The mixing ratios and the altitudes at which water ice clouds form are closer to observations than other GCM simulations. Other published models predicted mixing

ratios of ice clouds about 5 times higher than observed, and the cloud layers are located at lower levels (1 to 3 mb) over the northern tropics [Richardson *et al.*, 2002, Montmessin *et al.*, 2004], whereas in our model the ice cloud belt has a deep multiple-staged vertical structure with the upper stage extending above 0.4 mb to 0.06 mb. The latitudinal extent and thickness of tropical cloud belt is constrained by the degree of water transport and the vapor amounts. In early summer at 0.2 mb, the highest zonal average of mixing ratio over the northern tropics is about 6 ppm. The thick cloud layers stretch across the tropics and their mixing ratios increase up to 30 ppm throughout late summer.

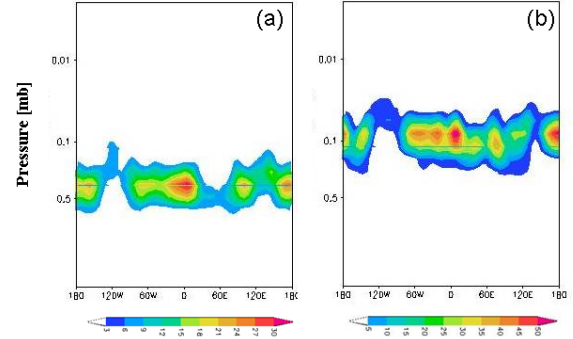


Figure 3: Longitudinal cross sections of ice clouds mixing ratios over the equator at (a)  $L_s = 119^\circ$  and (b)  $L_s = 160^\circ$

Figure 3 shows longitudinal cross sections of ice cloud mixing ratios over the equator at  $L_s = 119^\circ$  and  $160^\circ$ . The simulated high mixing ratios of the thick cloud layers vary much with longitude. There are ice layers at about 0.3 mb with high mixing ratios up to 30 ppm (Figure 3a) and other predicted thick layers formed at a pressure level between 0.06 mb and 0.1 mb (Figure 3b). The results are consistent with the MCS observations of clouds from a narrow latitude band centered on the northern tropic and intersecting Lycus Sulci and the Elysium Montes during summer of MY 28-29 [Heavens *et al.*, 2010].

## Conclusion

The study presents the seasonal variability of the  $H_2O$  vapor and ice clouds simulated with the MAOAM-GCM. The simulations are focused on validating the newly developed cloud parametrization scheme. The model results are consistent with recent observations of the Martian atmosphere, and compares well with other GCMs.

## References

- Becker, E., J. Atmos. Sci., 66, 647 (2009)
- Hartogh, P., Medvedev A., Kuroda, T., Saito, R., *et al.*, J. Geophys. Res., 110, E11008 (2005)
- Heavens, N., Benson, J, Kass, D. *et. al.*, J. Geophys. Res. Lett., 37, L18202(2010)
- McCleese, D.J. Heavens, N.G., Schofield J.T, *et al.*, J. Geophys. Res., 115, E003677(2010)
- Montmessin, F., Forget. F., Rannou, P., *et al.*, J. Geophys. Res., 109, 1029 (2004)
- Moudden, Y., McConnell. J., Icarus, 188, 18 (2007)
- Richardson, M. and Wilson, R.J. Geophys. Res., 107, 5031(2002)
- Smith, M., Pearl, J., Conrath, B. and Christensen, P. J. Geophys. Res. 106, 945 (2001)